

A model of synchronisation in crowd dynamics

Filippo GAZZOLA* – Vitomir RACIC†

Abstract

This study is motivated by the lack of adequate models of dynamic loading of civil engineering structures that are primarily occupied by active groups and crowds of people, such as footbridges, floors and grandstands. The primary objective is to develop a mathematical model of synchronisation of multiple people performing cyclic motion such as walking, running, jumping and bouncing. In conjunction with a quality model of individual loading, the sync model is the key ingredient needed to provide a reliable numerical generator of aggregate dynamic excitation of the supporting structure. The model describes the effect of periodic external cues on the crowd motion, such as perceptible vibration of the ground and a music beat, and the mutual interaction between individuals. The main feature of the model is that it is *linear and deterministic*, no randomness and no nonlinearity for the sake of simplicity and efficiency: it is inspired to models of coupled pendulums and the governing equations feature Mathieu-type behaviors. The modelling parameters have a physical interpretation and their values can be calibrated to potentially match experimental measurements.

Keywords: synchronisation, human-structure dynamic interaction, Hill equations, footbridges, floors.

AMS Subject Classification: 34A30, 34D06, 34B30.

1 Introduction

For vibration-sensitive structures such as footbridges, floors, staircases and grandstands, prediction of coordinated dynamic loads induced by groups and crowds of people presents a major challenge for design [1, 3, 18, 27, 44]. Meeting the challenge requires scientifically rational design guidance which can describe reliably human-induced loading. Despite quality models of individual loading do exist [6, 21, 29, 33, 34, 37, 41, 47], the true knowledge on how to expand them into models of group and crowd loading is still unknown [9, 24, 36]. A key missing element is a quality model of the interaction between multiple people during a cyclic (i.e. rhythmic) movement generally known as “synchronisation”. In the present paper we introduce a new mathematical model able to describe the human behavior through a number of parameters and to measure their synchronisation with a suitable sync function.

Available design guidance [7, 8, 16, 40, 22, 23] portrays a group of people as a set of identical robot-like force generators moving deterministically at a fixed frequency with either perfect synchronisation or random phases. Humans are not machines and natural variability and imperfect synchronisation point out to a random approach to describing their actions. Attempts to apply these state-of-the-art documents to real structures highlight the problems and uncertainties remaining [24, 43]. To date the limited body of research on the subject has been carried out by structural engineers with the aim of providing better guidance on multiple-occupant loads. Early studies on crowd rhythmic loads (e.g. jumping and bouncing) used a combination of direct laboratory measurement and Monte Carlo (MC) simulation [38]. The general approach was to collect data for individuals who were prompted to jump and bounce by means of an electronic metronome - the beat of which was recorded along with the loading data. Having fitted probability distributions of time lags between successive jumping/bouncing cycles and the prompt beat, the MC method of random sampling was used to generate the loads for a large group or crowd. However, the synthetic loads often generated smaller vibration responses when compared with the measured counterparts, indicating poorer synchronisation of

*Dipartimento di Matematica del Politecnico, Piazza L. da Vinci 32 - 20133 Milano (Italy)

†Dipartimento di Ingegneria Civile e Ambientale del Politecnico, Piazza L. da Vinci 32 - 20133 Milano (Italy)

movements between individuals than was actually occurring [15]. This is because peripheral stimuli, such as the possibility to see and/or hear each other, dramatically improve their coordination [28]. Hence, it is clear that synchrony between individuals is a complex process, dependent on multiple factors within the environment. More recent studies on walking loading [5, 43] focus on tracking body motion of multiple people on real structures to estimate the proportion of individuals in a given situation who coordinate their footfalls and the scale of the resulting net dynamic loads on the structure. Natural inability of individuals to keep the footfall rate constant (so called “intra-subject variability”) has been shown to make a great impact on the accuracy of the predicted vibration response [43, 45, 48]. Moreover, it was observed that strong synchronisation between individuals appears occasionally in scattered instances separated by intervals of weak or no synchronisation (see Figure 1).

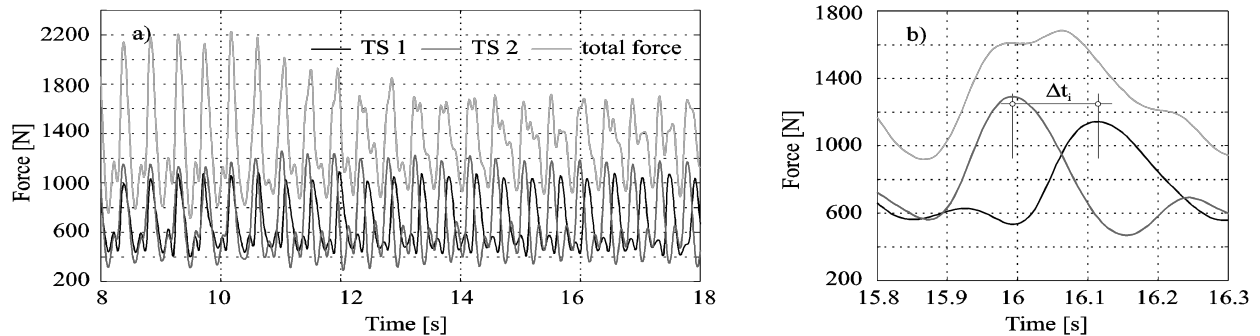


Figure 1: Ground reaction force due to a group of two bouncing people taken from [35]. Figures a) and b) represent the same data: Δt_i is the time difference between two local peaks.

However, explicit models of the synchronisation mechanism are very rare and limited [17, 32, 42, 45]. Some models are developed to describe the synchronisation phenomenon of specific events in nature, such as swarm behaviour, but are not directly applicable to humans. Others require large computational power and long simulation time, which makes them very unpopular among structural designers who normally work under a huge time pressure. The primary objective of this paper is to build a mathematical framework that can describe simply yet reliably synchronisation between multiple individuals who move while prompted by a periodic external stimulus. Examples include a music beat and strobe light in entertaining venues (e.g. concert halls), stadia and fitness centres, and perceptible structural vibration that affect the way people walk on footbridges. Small disturbances that can cause the “butterfly effect” [42], such as a bee distracting an individual leading to a wave of panic in the crowd, naturally lead to the introduction of random variables into the model. Nevertheless, occasional events *should not* be included into the model since they would lead to wrong hints for future plans and designs. Moreover, we do not take into account the nonlinear behavior of structures since this phenomenon becomes relevant only in presence of wide lateral movements of the structure [26]: for small movements, a linear model is sufficiently accurate. Finally, it should be stressed that the morphology of the synthetic individual trajectories is irrelevant as long as the required timing can be extracted. Bearing all this in mind, we introduce a model of a linear oscillator that generates superficial trajectories of the body motion for each individual in a group while prompted by a stimulus. Disturbance terms are added to the traditional deterministic equations of motion in Section 2, so individuals do not act as perfect oscillators. The group model is defined in Section 3 where we also introduce a “measure for sync”, see the function $A(t)$ in (6). Overall, our model simulates the combined effect of an external stimulus and inter-personal interaction using the analogy with a double pendulum and, hence, it gives rise to Mathieu-type equations [31, 39] which are just a particular case of the Hill equations [20, 30]. For these equations, random values of the modelling parameters are obtained by replacing constant coefficients within the classical pendulum equation with periodic functions. It is well-known that the solutions to these equations may show resonances and instability for certain values of the modelling parameters [12]. Nonlinear forms of these equations have been successfully used to analyse the stability of suspension bridges due to several interactive vibration sources [2, 17, 19] and possible resonances have been highlighted [4]. Even if the model elaborated

in the present paper features a simpler (yet reliable) linear form of the Mathieu-type equations, the resonances and instability still could happen. To avoid these unwanted effects, the individual parameters must be selected with extreme care, as shown in Section 4: in this section, we also show how these parameters influence both the behaviour of two individuals and of their global sync. In Section 5 we validate our results for two individuals by comparing them with results recorded in the Light Structures Laboratory at the University of Sheffield. Finally, the influence of the parameters is studied in the case of more individuals in Section 6. Some concluding remarks are drawn in Section 7.

2 Individual body motion

We consider the body motion $x_i = x_i(t)$ ($i = 1, \dots, n$) of an individual in a group of n people to be prompted by a periodic external stimulus $y = y(t)$ whose beat can be described by a simple pendulum equation:

$$\ddot{y} + \omega^2 y = 0. \quad (1)$$

The individuals are trying to sync their motion with the beat frequency ω . The difference $y_i = x_i - y$ describes how well each of them is doing. If individuals were perfect oscillators, the difference would gradually approach zero and remain zero unless disturbed further. This ideal condition can be modelled by the following damped linear differential equation:

$$\ddot{y}_i + 2\varepsilon\dot{y}_i + (\varepsilon^2 + \alpha^2)y_i = 0, \quad (2)$$

where ε is a measure of the tendency to synchronise while α is the frequency of the body motion. The general solution of (2) is given by

$$y_i(t) = e^{-\varepsilon t} (A \cos \alpha t + B \sin \alpha t) \quad (A, B \in \mathbb{R})$$

that describes oscillations of frequency α which is damped for increasing t . For large ε the difference y_i becomes smaller earlier, showing a stronger tendency to sync between the individual x_i and the beat y . This simple model is the starting point for the further discussion and the model advancement that follows. In the real world individuals come in different shapes and forms and human behavior is inherently heterogeneous. Also, they show irregular cyclic motion due to the intrinsic inability to repeat exactly the same move (i.e. intra-subject variability). This suggests that ε and α in (2) should be personalised: $\varepsilon = \varepsilon_i$ and $\alpha = \alpha_i$. Individual i synchronises better with the beat than individual j if $\varepsilon_i > \varepsilon_j$, while $\alpha_i > \alpha_j$ means that individual i moves “faster” than individual j . Hence, it appears reasonable to replace the constants ε and α^2 in (2) with some variable and slightly oscillating functions depending on a personal frequency-parameter ω_i :

$$\varepsilon \longrightarrow \varepsilon_i(\delta_i + \sin \omega_i t), \quad \alpha^2 \longrightarrow \omega^2(1 + \gamma_i \sin \omega_i t). \quad (3)$$

Here, *intra-subject variability is assumed to be a periodic activity with frequency $\omega_i > 0$* , i.e. the rate by which an individual modifies his/her motion with respect to the given beat, while γ_i controls the intensity of the variation. For instance, higher values of both parameters can describe a person tense with excitement. Numerical simulations suggest that the value of ω_i should differ from ω by at least 3% to avoid the resonance: this problem is clearly due to the double pendulum model (Mathieu-type equations display such resonances, see [12, 31, 13]) and appears when the frequencies are too close to each other. However, this assumption is perfectly in line with real life: in order to avoid resonances, structures subject to human-induced forces are nowadays planned stiff enough to move their natural frequency out of the range that could be excited by these forces. This may be achieved either by increasing the total mass or by adding extra structural elements or by adding tune mass dampers at the design stage.

The offset δ_i accounts for the interaction between individual i and others, e.g. a possibility to see people around. There is no interaction when $\delta_i = 0$. As the synchronisation generally improves with close interactions between individuals [9, 10, 11, 14, 24], δ_i needs to be positive so the individual moves closer to the beat. On the other hand, the condition $\delta_i < 1$ yields positive and negative values in the overall damping ε in

(2). In this way, distinct levels of the difference y_i could be simulated most effectively. Combining (2), (3) leads to:

$$\ddot{y}_i + 2\varepsilon_i(\delta_i + \sin \omega_i t)\dot{y}_i + (\varepsilon_i^2(\delta_i + \sin \omega_i t)^2 + \omega^2(1 + \gamma_i \sin \omega_i t))y_i = 0. \quad (4)$$

As $y_i = x_i - y$, the equations of motion of the individuals can be derived from (4):

$$\ddot{x}_i + \omega^2 x_i + 2\varepsilon_i(\delta_i + \sin \omega_i t)(\dot{x}_i - \dot{y}) + (\varepsilon_i^2(\delta_i + \sin \omega_i t)^2 + \omega^2 \gamma_i \sin \omega_i t)(x_i - y) = 0. \quad (5)$$

This yields a set of n independent equations (for $i = 1, \dots, n$), each featuring the body motion of a single individual. The link with the rest of the group is modelled via the beat y and parameter δ_i , which spreads the interaction evenly within the group. However, the strongest interaction is expected with the neighboring people and even at different levels with different neighbors depending on their positions. For instance, in case of a visual stimulus an individual is affected more by persons moving in front than beside them, while there is no interaction with those behind. Still, adding any further conditions or constrains to (5) would lead to an unsolvable system of equations. To address the challenge, the next section introduces a ‘‘synchronisation function’’ which examines and bonds all possible couples within the group.

3 Synchronisation function

A time measure of the average (lack of) synchronisation $A(t)$ in a group of n people can be expressed as

$$A(t) = \frac{2}{n(n-1)} \sum_{i=1}^n \sum_{j=i+1}^n (\ddot{x}_i - \ddot{x}_j)^2 \geq 0 \quad (6)$$

where the (binomial) coefficient $2/n(n-1)$ is needed to compute the *average* among all possible couples of individuals. In the simplest case $n = 2$, this coefficient equals 1. If $A(t) = 0$ then all individuals in the group are moving in unison, while larger amplitudes of $A(t)$ indicate poor synchronisation within the group. Equation (6) deliberately features acceleration signals \ddot{x}_i and \ddot{x}_j as wireless accelerometers that are the state-of-the-art technology for tracking body motion on real civil engineering structures [5, 43]. This is particularly important for calibrating values of the modelling parameters in future using an adequate set of experimental data, which is currently not available in the literature.

As we shall see, all the phenomena are already visible when the crowd is reduced to $n = 2$ individuals. In this case, we may take advantage of the low number of involved parameters in order to give a physical interpretation of their role. Therefore, in Sections 4 and 5 we restrict our attention to the case $n = 2$, while in Section 6 we briefly comment the extension of the results to the case of more individuals.

In the case of two individuals ($n = 2$) the equation governing the interaction is obtained by subtraction of the equations (5):

$$\begin{aligned} & (\ddot{x}_1 - \ddot{x}_2) + \omega^2(x_1 - x_2) \\ & + 2\varepsilon_1(\delta_1 + \sin \omega_1 t)\dot{x}_1 - 2\varepsilon_2(\delta_2 + \sin \omega_2 t)\dot{x}_2 \\ & + (\varepsilon_1^2(\delta_1 + \sin \omega_1 t)^2 + \omega^2 \gamma_1 \sin \omega_1 t)x_1 - (\varepsilon_2^2(\delta_2 + \sin \omega_2 t)^2 + \omega^2 \gamma_2 \sin \omega_2 t)x_2 \\ & + 2(\varepsilon_2(\delta_2 + \sin \omega_2 t) - \varepsilon_1(\delta_1 + \sin \omega_1 t))\dot{y} \\ & + (\varepsilon_2^2(\delta_2 + \sin \omega_2 t)^2 + \omega^2 \gamma_2 \sin \omega_2 t - \varepsilon_1^2(\delta_1 + \sin \omega_1 t)^2 - \omega^2 \gamma_1 \sin \omega_1 t)y = 0, \end{aligned} \quad (7)$$

where each line has a different meaning. If we denote by $x_{1,2} = x_1 - x_2$, then the first line in (7) contains the usual terms of the pendulum equation for $x_{1,2}$: if it equals 0 then one has the harmonic oscillator with frequency ω which is precisely the behaviour of the beat, see (1). The second and third lines in (7) contain the perturbation terms due to the specific behaviour of the individuals x_1 and x_2 ; they depend on all the above described characteristic parameters. Finally, the last two rows in (7) act as a forcing term to the difference $x_{i,j}$: they depend only on the stimulus y and on the characteristic parameters of each individual but do not depend explicitly on the individuals x_i and x_j themselves. Therefore, this is the part where synchronisation

comes into the model, that is, when the parameters ε and δ are involved. Increasing the former yields a stronger “damping term”, that is a stronger synchronisation with the stimulus and, as a byproduct, a stronger synchronisation between individuals. But, as we shall see, the relevant parameter for a better synchronisation between the individuals without taking into account the indirect influence of the beat is δ .

4 Influence of modelling parameters on synchronisation function

In the following two sections we plot the graph of the sync function $A(t)$ defined in (6): we consider the case $n = 2$ and we introduce different values of the parameters. All the plots are obtained by using the software Mathematica. In each of the following four subsections, values of a single modelling parameter are varied for one or both persons to illustrate qualitatively the effect this produces on the synchronisation function $A(t)$ in (6). Other parameters are kept constant but not necessarily at the same baseline (nominal) level across all the subsections. There are two reasons for doing this. Firstly, some combinations of the parameter values cause instability of the solution, which is the nature of the Mathieu equations and functions elaborated in Section 4.3. Similar behavior can be observed in resonant vibration response of lightly damped structures [18, 29] or in general Hamiltonian systems [4]. Secondly, in each subsection the values of the parameters are chosen carefully to illustrate best different morphologies that the synchronisation function $A(t)$ can take due to the variations of a target parameter. Although experimental data are needed to validate the selected values, the angular frequency of the stimulus $\omega = 4\pi\text{rad/s}$ is adopted in all subsections. It corresponds to 2Hz, which is widely reported as the most comfortable (thus the most common) rate of the cyclic body motion for the majority of people [24, 34]. Symbols P_1 and P_2 stand for Person 1 and Person 2, respectively.

4.1 Parameter ε_i

Four simulations are carried out for different values of ε_1 , while ε_2 is kept fixed. The values of all modelling parameters used in the simulations are given in Table 1 and the results are shown in Figures 2 and 3. The frequencies ω_i are expressed in rad/s so that $\omega_1 \approx 1.6\text{Hz}$ which is in the range of common frequencies for walking, usually expected in the range 1.5-2.5Hz. The value of $\omega_2 \approx 0.32\text{Hz}$ is unnaturally low but it was selected to demonstrate best performance of the model.

i	1	2
a) ε_i	0.01	0.001
b) ε_i	0.1	0.001
c) ε_i	0.8	0.001
d) ε_i	-0.2	0.001

i	1	2
δ_i	0.08	0.008
γ_i	0.8	0.8
ω_i	10	2

Table 1: Values of the parameters for Figures 2 and 3.

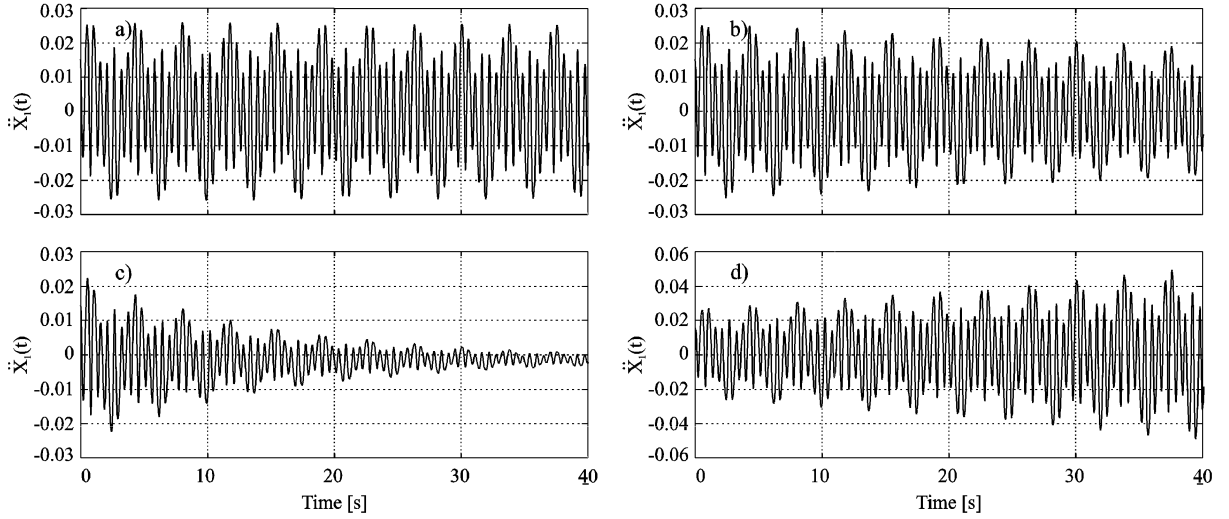


Figure 2: Acceleration trajectories of P_1 (Figure d) has half of the vertical scale).

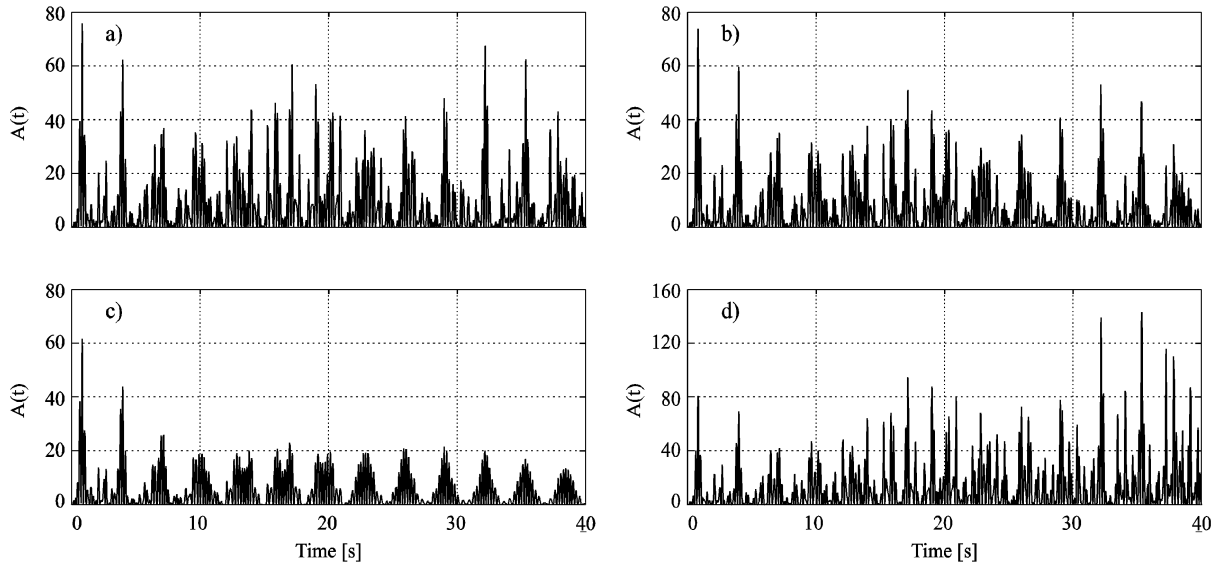


Figure 3: The function $A(t)$ due to variations of ε_i (Figure d) has half of the vertical scale). The corresponding values of the modelling parameters are given in Table 1.

According to (7), increasing ε_1 yields a stronger damping term (the second line), which means a stronger synchronisation of P_1 with the stimulus (Figure 2, pictures a-c)) and as a byproduct a stronger synchronisation between the individuals (Figure 3, pictures a-c)). Negative values of ε_1 have the opposite effect. They intensify the motion of P_1 (Figure 2, picture d)) leading to poorer synchronisation of the group (Figure 3, picture d)).

4.2 Parameter δ_i

The δ_i -parameters define intensity of the inter-personal interaction without the influence of the stimulus. Figure 4 shows the synchronisation function $A(t)$ due to different combinations of δ_1 and δ_2 reported in Table 2. Case a) takes a large value of δ_1 while δ_2 is kept very low. Case b) brings them to the same high level, followed by a reduction of δ_1 by half in case c). Finally, both δ_1 and δ_2 take equal and small values in case d).

At the first glance, the plots seem identical, thus demonstrate how little $A(t)$ -amplitudes are sensitive to

the variations of the δ_i . When compared to the results in Figure 4, it is apparent that the model gives a more important role to the stimulus than to the influence of the surrounding people on the body motion of individuals. This is exactly what was already reported in the literature for walking, jumping and bouncing [14, 29]. To illustrate the impact of various δ_i -values, the plots b-a), c-a), d-a) in Figure 5 show, respectively, the difference between the plots b), c), d) and the plot a) presented in Figure 4. As expected, by increasing $\delta_1 + \delta_2$ the synchronisation improves (the function $A(t)$ decreases) while it gets worse (the function $A(t)$ increases) as $\delta_1 + \delta_2$ decreases. Note that two different combinations of δ_1 and δ_2 but having the same sum cannot yield the same $A(t)$ as the other parameters describing the two persons are not the same.

i	1	2
a) δ_i	0.08	0.008
b) δ_i	0.08	0.08
c) δ_i	0.04	0.08
d) δ_i	0.01	0.01

i	1	2
ε_i	0.001	0.001
γ_i	0.8	0.8
ω_i	10	2

Table 2: Values of the parameters for Figure 4.

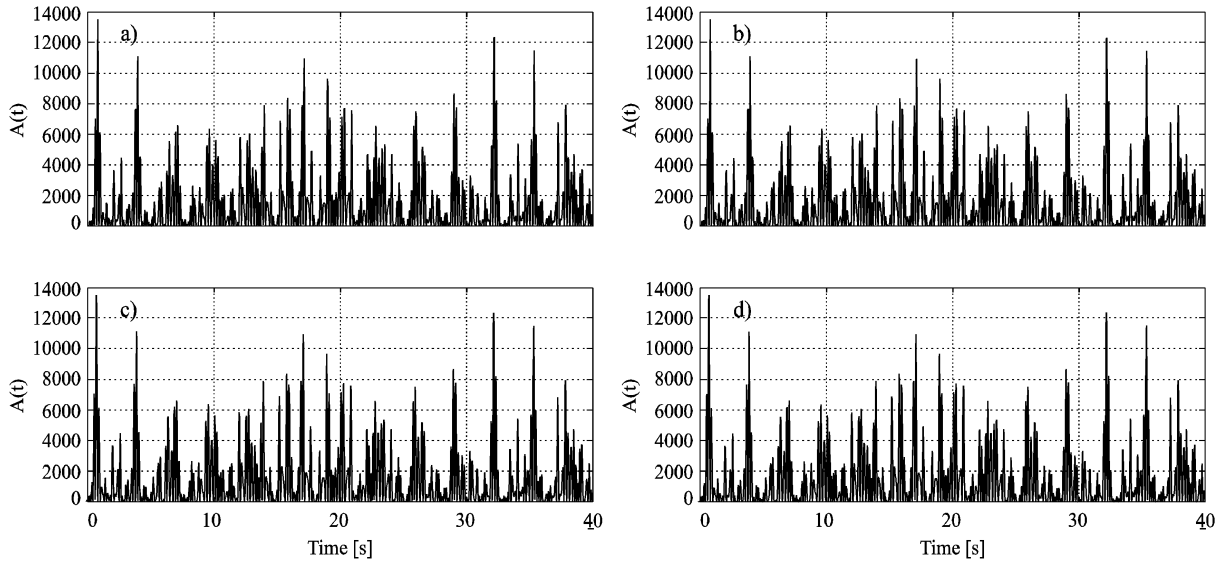


Figure 4: The function $A(t)$ due to variations of δ_i . The corresponding values of the modelling parameters are given in Table 2.

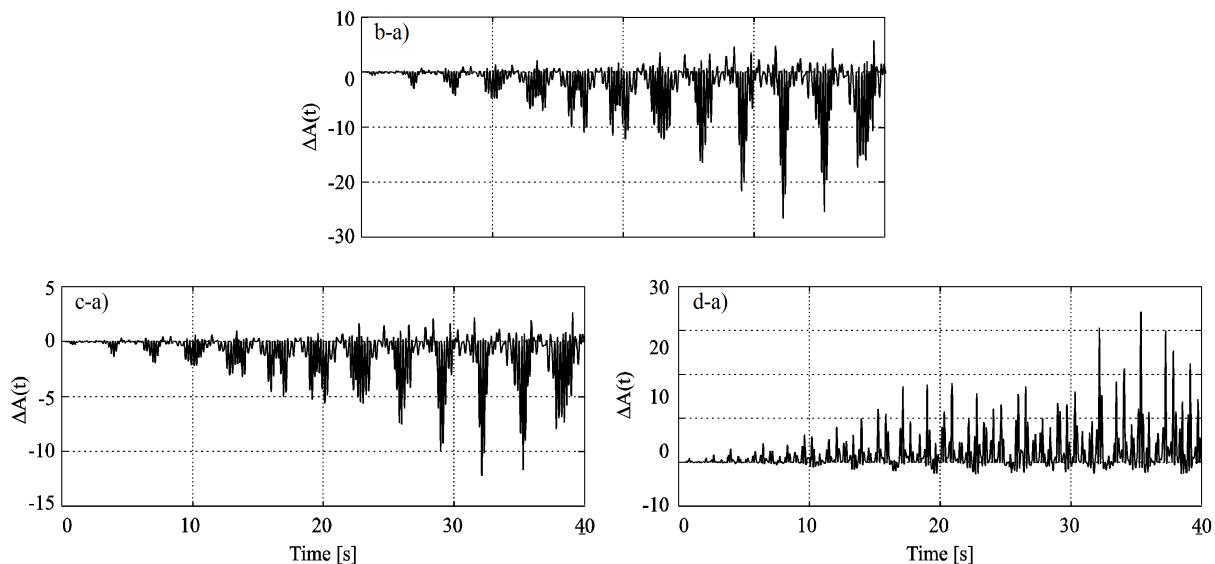


Figure 5: Differences between the plots b), c), d) and the plot a) of the $A(t)$ -curves shown in Figure 4.

As already mentioned above, not all of the modelling parameters are mutually independent. The next section reveals why the values of ω_i and γ_i cannot be selected randomly and independently.

4.3 Link between ω_i and γ_i

There is an analogy between (7) and the following Mathieu equation:

$$\ddot{\xi}(t) + (a + 2q \cos 2t)\xi(t) = 0, \quad (a, q \in \mathbb{R}). \quad (8)$$

Here, $\xi = \xi(t)$ is a time variable while a and q are constants. It is well-known [12, 31] that there exists couples of values (q, a) for which the trivial solution $\xi \equiv 0$ of (8) is stable or, equivalently, for which all the solutions of (8) are bounded in \mathbb{R} . The stability analysis for (8) is well-understood: in the (q, a) -plane, the resonance tongues (or instability regions) for (8) emanate from the points $(0, \ell^2)$, with $\ell \in \mathbb{N}$, see Figure 6 where the resonance tongues are shaded in gray while the stability regions are white.

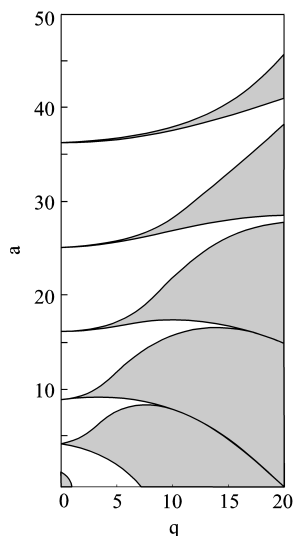


Figure 6: Stability regions (white), resonance tongues (gray) for (8) in the (q, a) -plane.

Hence, the values of the parameters a and q in (8) should be selected with extreme care. It appears clearly from Figure 6 that, in order to remain into a stability region, the parameters q and a may be modified only following suitable patterns and that they depend on each other. With the lunar perigee model by Hill [20], if these parameters exit the stability regions, this would mean that the moon would leave the orbit of the earth!

A precise picture as Figure 6 cannot be plotted for (4) due to its complexity. However, stability of the solutions can be studied by running numerical simulations where ω_i and γ_i are varied in very small steps. Figure 7 illustrates how sensitive the problem is. It presents $A(t)$ calculated for two sets of the parameters having different only γ_2 values, i.e. -1 (top) and -1.01 (bottom). It is apparent that despite the minute difference the solutions are dramatically different.

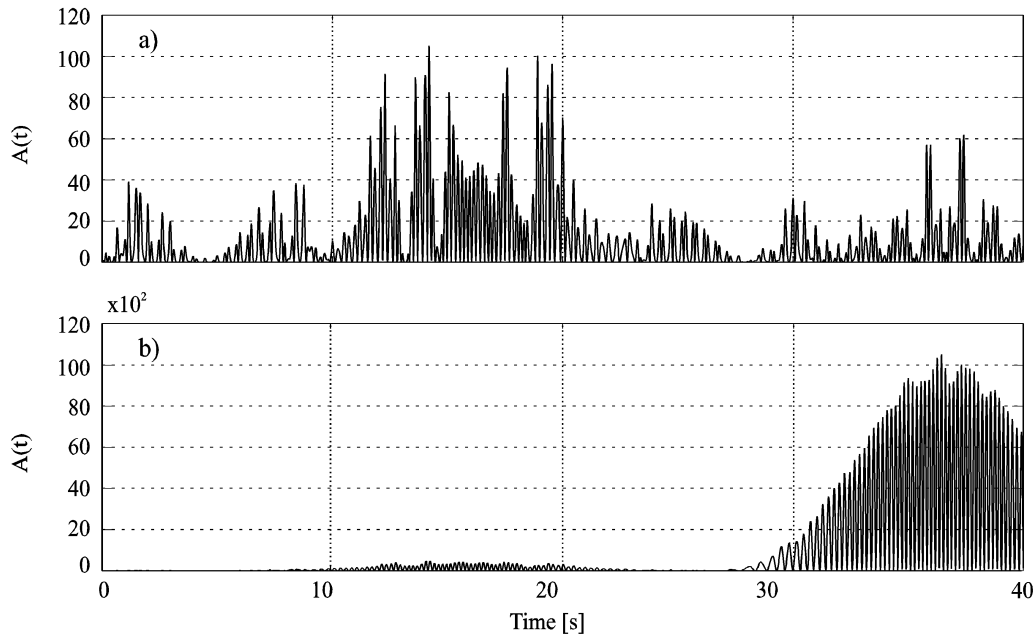


Figure 7: Example of extremely different $A(t)$ due to a small variation of γ_2 : a) stable solution and b) unstable (blowing up) solution.

The next two subsections proceed with illustrations of the impact of varying γ_i and ω_i on the synchronization function $A(t)$ in the same manner as it was done in Sections 4.1 and 4.2 for the other two parameters.

4.4 Parameter γ_i

The parameter γ_i stands for the amplitude of the intra-subject variation. Small values in the range $(-1, 1)$ are expected for the majority of people since the inborn ability to follow well a rhythm is what sets apart the majority of humans from other creatures on the planet. Values outside this range would describe those rare individuals, so called “beat deaf” persons, to whom a rhythm does not come naturally thus cannot move in time with it. In small groups, such as pairs studied here, they can even obstruct the motion of others.

Concerning the parallel with the Mathieu equations, sign and amplitude of γ_i greatly influence the stability of $A(t)$. The thresholds -1 and 1 appear critical as small perturbations can give rise to a blow up of $A(t)$, as illustrated in Figure 7. However, this should not be taken as a rule. The values of γ_i outside the range still could provide stable solutions depending on the values of the corresponding ω_i . Figure 8 shows $A(t)$ simulated using values of the modelling parameters in Table 3.

i	1	2
a) γ_i	0.8	0.8
b) γ_i	0.8	0.4
c) γ_i	0.8	0.2
d) γ_i	0.9	0.1

i	1	2
ε_i	0.001	0.001
δ_i	0.08	0.008
ω_i	10	2

Table 3: Values of the parameters for Figure 8.

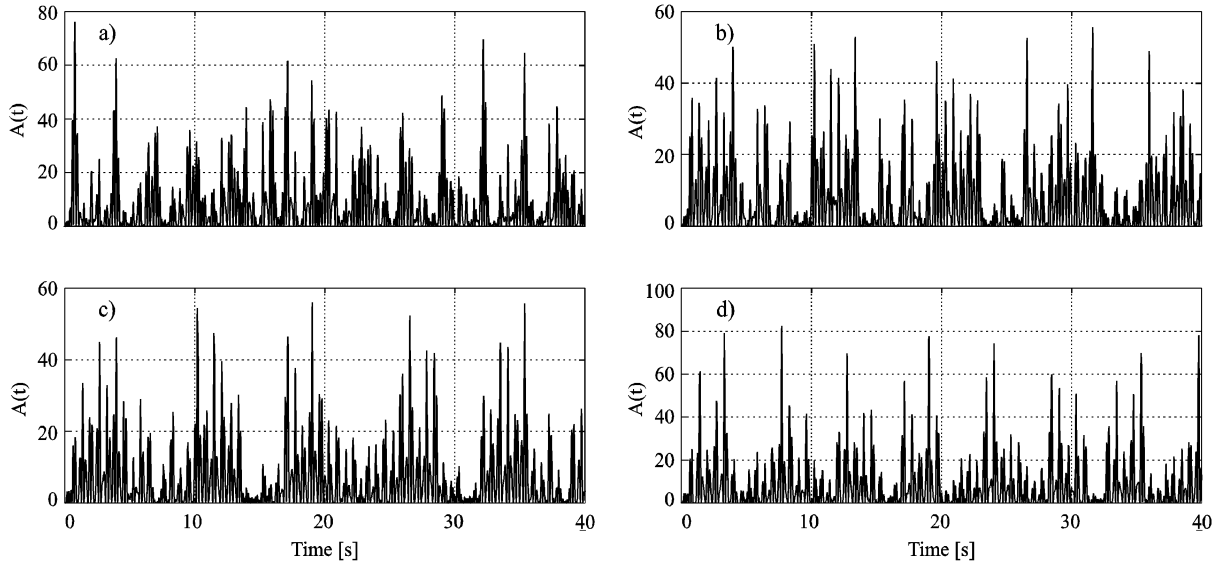


Figure 8: The function $A(t)$ due to variations of γ_2 . The corresponding values of the modelling parameters are given in Table 3.

4.5 Parameter ω_i

Low values of ω_i correspond to “calm” individuals who need time to synchronise with the beat of the stimulus but stay synchronised over long periods. In contrast, high ω_i values describe “frantic” persons who pick up and lose the beat quickly. Table 4 contains four combinations of ω_i -values that yield four different shapes of $A(t)$, reported in Figure 9. In the first two cases the values of ω_i are very different and ω_2 is very small. The remaining two cases take both ω_i with values large, firstly close to each other (picture c) in Figure 9) and then apart (picture d) in Figure 9). These four cases show that couples with similar ability to follow the given beat synchronise more frequently. How long they are going to stay in sync depends on the frequency of the beat and on the rate of their variation with respect to the beat. On the other hand, significantly different ω_i -values yield irregular $A(t)$ characterised by clear succession of sync and non-sync clusters.

i	1	2
a) ω_i	16	0.2
b) ω_i	1.5	0.2
c) ω_i	16	14
d) ω_i	34	16

i	1	2
ε_i	0.001	0.001
δ_i	0.08	0.008
γ_i	0.8	0.8

Table 4: Values of the parameters for Figure 9.

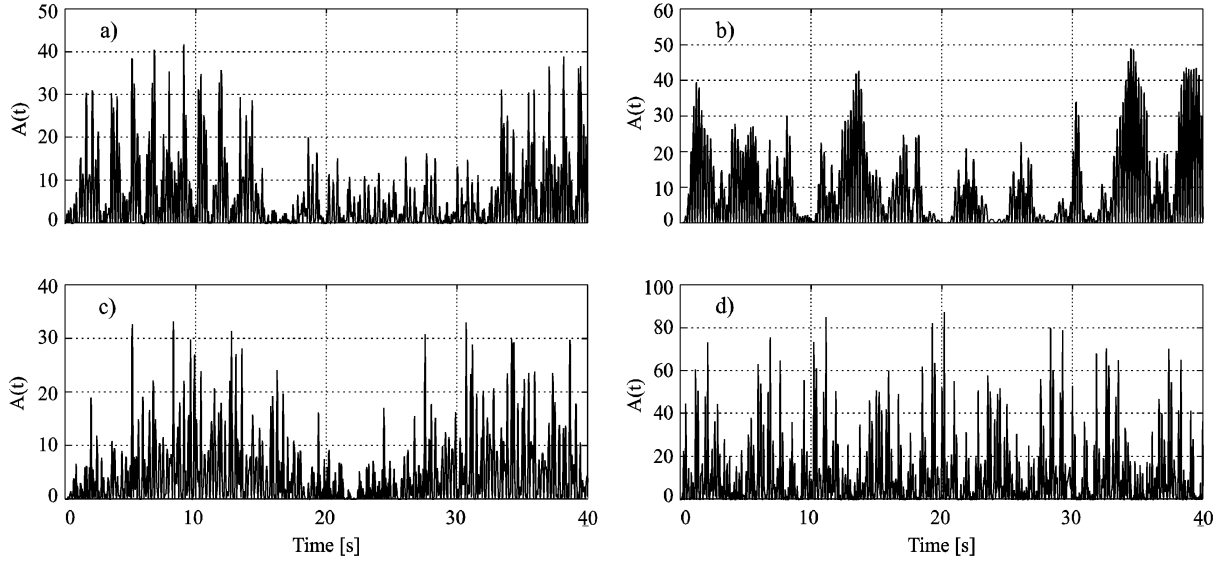


Figure 9: The function $A(t)$ due to variations of ω_i . The corresponding values of the modelling parameters are given in Table 4.

5 Validation of the model

Some real body motion data have been recorded in the *Light Structures Laboratory at the University of Sheffield*: the experimental setup and the data collection are elaborated in [35]. We aim here to check whether these experimentally recorded data fit in our theoretical model. Our goal is to show that with a suitable choice of the parameters in (7) we are able to reproduce what was measured in reality. To this end, we consider again the measure of synchronisation defined in (6).

Two activities have been measured: bouncing and jumping. During bouncing, the pelvis moves up and down with the flexed knees, but the feet never leave the ground. For instance, this is close to what happens when people are “dancing” while listening a song. Jumping has “flying” phases, the feet of the individuals leave the ground in some intervals of time. Jumping is a more vigorous activity than bouncing and can often be observed during rock concerts and sport events: this is a very particular and not well known situation.

In the next five figures, we compare real behaviour of humans (left picture, extrapolated from the data in [35]) with the solutions of (7) for a suitable choice of the parameters (right picture). In both cases, we plot the function A in (6) with $n = 2$. In all the numerical experiments, the interval of time integration was $[0, 40]$.

We compare three examples for people bouncing. For the first example (Figure 10), the frequency of body motion is 2.3Hz while the parameters in (7) are

$$\omega = 14.451; \omega_1 = 23.12; \omega_2 = 5.78; \varepsilon_1 = 0.001; \varepsilon_2 = 0.01; \delta_1 = 0.008; \delta_2 = 0.008; \gamma_1 = 0.75; \gamma_2 = -0.1.$$

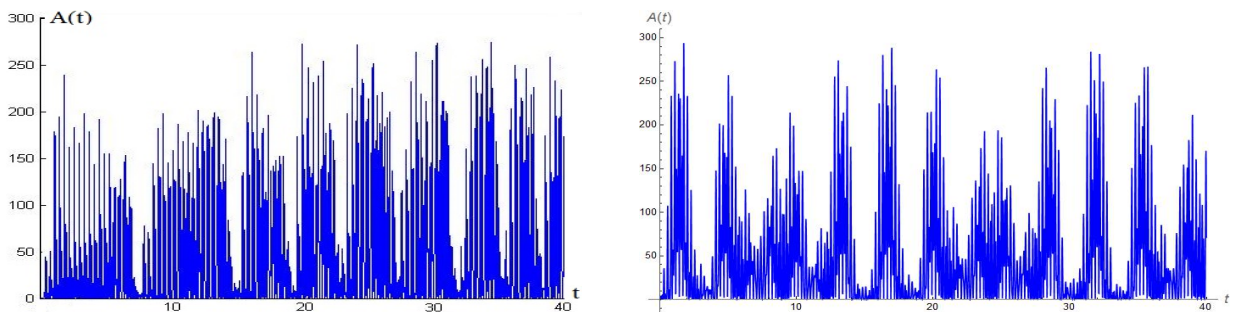


Figure 10: First example of comparison of $A(t)$ for 2 persons bouncing.

For the second example (Figure 11), the frequency of bouncing is $2Hz$ while the parameters in (7) are $\omega = 12.566$; $\omega_1 = 37.698$; $\omega_2 = 20.106$; $\varepsilon_1 = 0.001$; $\varepsilon_2 = 0.01$; $\delta_1 = 0.8$; $\delta_2 = -0.07$; $\gamma_1 = 0.6$; $\gamma_2 = 0.3$.

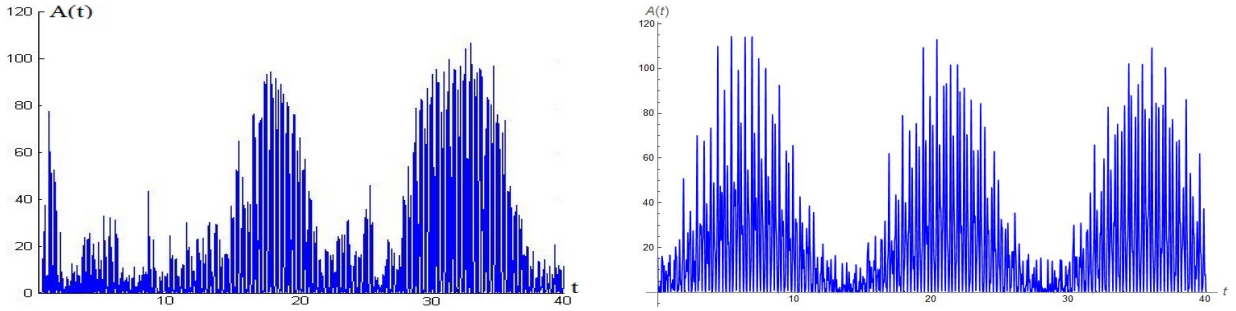


Figure 11: Second example of comparison of $A(t)$ for 2 persons bouncing.

For the third example (Figure 12), the frequency of bouncing is $3.5Hz$ while the parameters in (7) are $\omega = 21.991$; $\omega_1 = 26.389$; $\omega_2 = 0.22$; $\varepsilon_1 = 0.001$; $\varepsilon_2 = -0.001$; $\delta_1 = 0.08$; $\delta_2 = 0.008$; $\gamma_1 = 0.8$; $\gamma_2 = -0.3$.

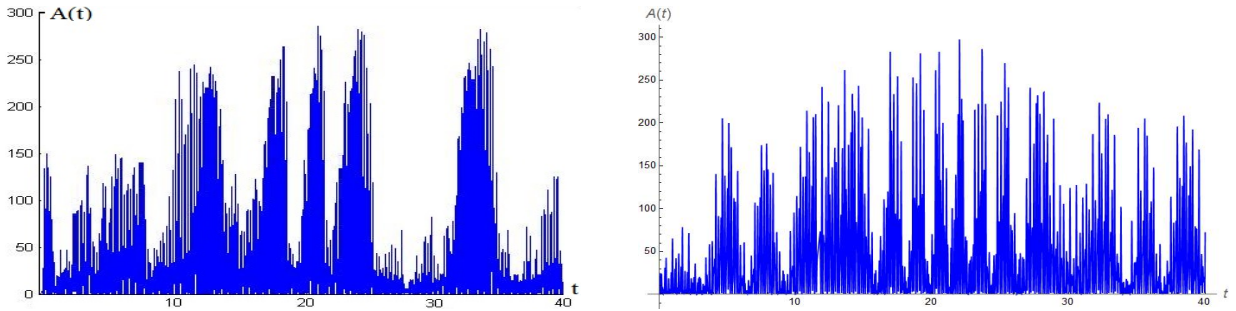


Figure 12: Third example of comparison of $A(t)$ for 2 persons bouncing.

The two following examples of jumping have the same time integration $[0, 40]$ as in case of bouncing. For the first example (Figure 13), the jumping frequency is $2.2Hz$ and the parameters in (7) are fixed to

$\omega = 13.823$; $\omega_1 = 22.117$; $\omega_2 = 19.352$; $\varepsilon_1 = -0.001$; $\varepsilon_2 = 0.01$; $\delta_1 = 0.008$; $\delta_2 = 0.008$; $\gamma_1 = 0.7$; $\gamma_2 = -0.1$.

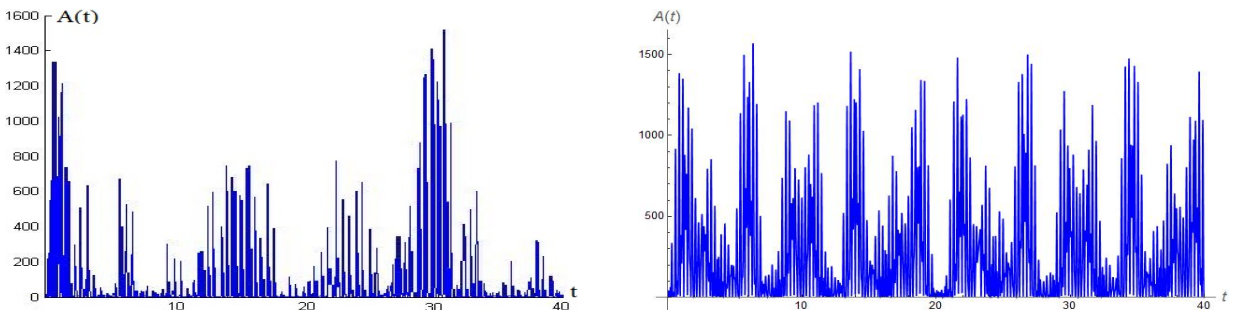


Figure 13: First example of comparison of $A(t)$ for 2 persons jumping.

For the second example (Figure 14), the jumping frequency is $2.5Hz$ and the parameters in (7) are fixed to $\omega = 15.708$; $\omega_1 = 23.562$; $\omega_2 = 1.571$; $\varepsilon_1 = 0.001$; $\varepsilon_2 = -0.01$; $\delta_1 = -0.08$; $\delta_2 = 0.008$; $\gamma_1 = 0.4$; $\gamma_2 = 0.3$.

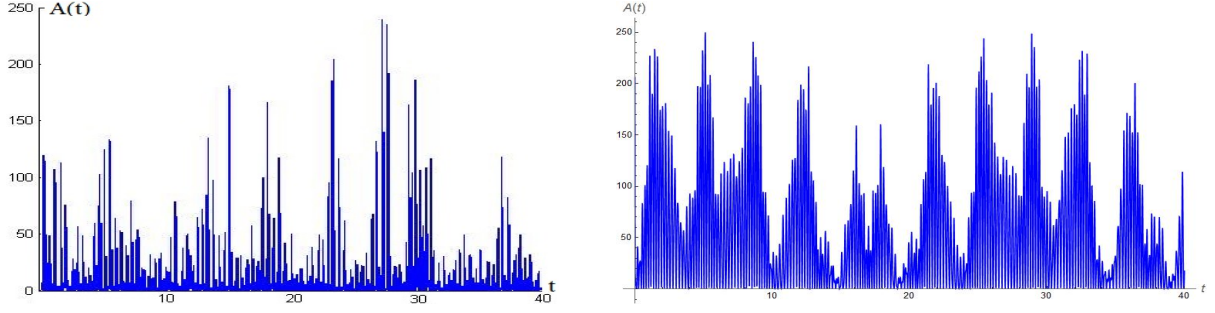


Figure 14: Second example of comparison of $A(t)$ for 2 persons jumping.

Overall, the above figures show that a suitable choice of the parameters in (7) leads to a reliable reproduction, at least qualitatively, of the sync function for a real couple of individuals. Hence, these figures show that (7) may allow to predict the sync between two individuals, provided that the frequency of the beat is known.

6 The case of a crowd

In this section we partially extend the results and remarks obtained in Section 4 to the case of $n = 10$ individuals. In fact, we also obtained similar results for more individuals (up to $n = 20$) with no significant changes in the response of our model.

As we have seen in Section 4.1, the ε_i are damping parameters. Their effect is visible on each individual (see Figure 2) and the same occurs for any number n of individuals. Again we point out that stronger damping parameters yield stronger synchronisations of the individuals with the beat and, as a consequence, between each other. There are no substantial differences for larger $n \geq 2$.

Next, we considered two groups of $n = 10$ individuals both having the same parameters except for the δ_i . We took

$$\omega = 12, \omega_1 = \omega_4 = \omega_7 = \omega_{10} = 1, \omega_2 = \omega_5 = \omega_8 = 1.5, \omega_3 = \omega_6 = \omega_9 = 2, \quad (9)$$

$$\varepsilon_1 = \varepsilon_6 = 0.001, \varepsilon_2 = \varepsilon_7 = 0.002, \varepsilon_3 = \varepsilon_8 = 0.003, \varepsilon_4 = \varepsilon_9 = 0.004, \varepsilon_5 = \varepsilon_{10} = 0.005, \quad (10)$$

$$\gamma_1 = \gamma_3 = \gamma_5 = \gamma_7 = \gamma_9 = 0.7, \gamma_2 = \gamma_4 = \gamma_6 = \gamma_8 = \gamma_{10} = 0.8, \quad (11)$$

for both groups. Then we took

$$\delta_1 = \delta_2 = \delta_3 = \delta_4 = \delta_5 = 0.08, \delta_6 = \delta_7 = \delta_8 = \delta_9 = \delta_{10} = 0.008, \quad (12)$$

for the first group (so that $\sum_{i=1}^{10} \delta_i = 0.44$) and

$$\delta_1 = 0.08, \delta_2 = \delta_4 = 0.07, \delta_3 = \delta_5 = \delta_6 = \delta_7 = \delta_8 = \delta_9 = \delta_{10} = 0.09,$$

for the second group (so that $\sum_{i=1}^{10} \delta_i = 0.85$). Note that even if the sum of the δ_i of the second group is larger, not all the δ_i (individually) are larger than the corresponding δ_i of the first group. We solved the system (5) and we computed the function A in (6) for both groups. In Figure 15 we display the plot of the difference $B(t)$ between the function A of the first group (which has a smaller $\sum_i \delta_i$) and the function A of the second group.

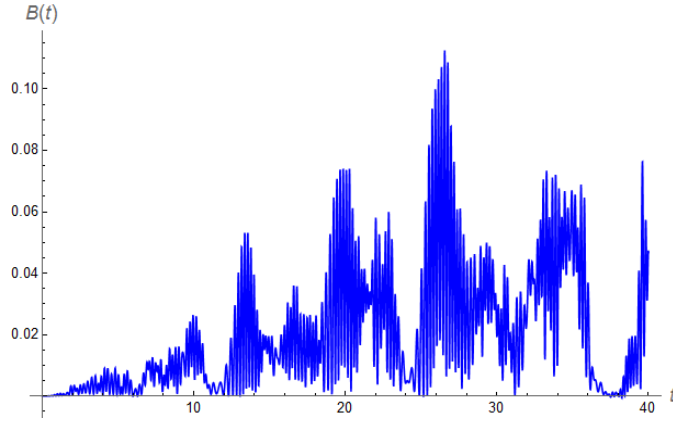


Figure 15: Comparison of $A(t)$ -functions for different groups of individuals.

It turns out that B is positive, thereby confirming the principle that *the synchronisation between individuals increases for decreasing $\sum_i \delta_i$* . The only difference between the case with only $n = 2$ individuals is that the behavior appears less regular: Figure 15 should be compared with the plots in Figure 5. Let us also mention that we obtained the same qualitative behavior of B and we reached the same conclusions also for other choices of the parameters, thereby proving that our model is robust.

As already mentioned, the parameter γ_i stands for the amplitude of the intra-subject variation and the stability range seems to be $(-1, 1)$, or some small variations of it. Outside this range one should expect instability of $A(t)$, in the spirit of the Mathieu equations. The same phenomenon is observed for groups of $n = 10$ individuals.

In Figure 16 we compare the A -function between two groups where only the parameter γ_2 is modified. The parameters used are the same as in (9)-(10)-(11)-(12) except that we took $\gamma_2 = 1$ for the first group (left picture) and $\gamma_2 = 1.03$ (right picture) for the second group.

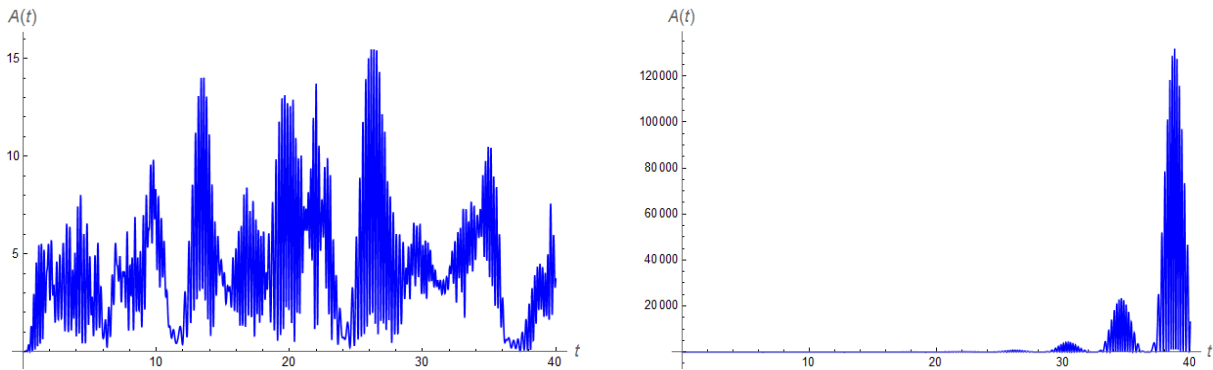


Figure 16: Comparison of $A(t)$ -functions for slightly different values of γ_2 .

Note the large "bump of asynchronisation" appearing in the second picture. We increased further γ_2 and the bump became considerably higher, for $\gamma_2 = 1.1$ it was already of the order of 10^{18} . These results fully confirm what was already emphasized for the simpler case $n = 2$.

Finally, let us mention that also the parameters ω_i (describing the ability to follow the beat) highlighted the same phenomena already visible for $n = 2$. Their variation slightly modifies the range of admissible γ_i . Moreover, groups with similar abilities (close enough ω_i) synchronise more frequently while significantly different abilities (spread ω_i) yield irregular sync functions $A(t)$ with evident successions of sync and non-sync clusters.

7 Discussion and conclusions

This study presents a mathematical model that describes coordination of the body motion within a group of individuals moving in the presence of an external periodic stimulus. Apart from a tendency (or the lack of it) of each individual to keep moving with the beat of the stimulus, the model proposed also takes into account the mutual interaction between the individuals. The model recognizes each person as an oscillator whose motion is unique, which helps to simulate different coordination scenarios within the group. According to the second Newton's law, the source of the dynamic loading generated by active people is in the body motion. Hence, the artificially generated motion trajectories of individual group members can be used to extract relative timing or phase shifts between the corresponding individual force time histories. These can be used in a conjunction with a model of individual loading (which depends on the activity) to generate a signal of the net dynamic loading due to the entire group. Individual loading models that can generate artificial forces on the cycle-by-cycle bases [25, 33, 37, 44] are the ideal candidates. This novel approach to modelling dynamic excitation of civil structures due to multiple active people is more realistic than the models featuring the relevant design guidelines, which commonly describe only two extreme situations - a full synchronisation or its absence. The key mathematical novelty is describing the random behavior of individuals by the *linear deterministic equation of a pendulum with enough uncertainty to simulate reliably the actual behavior of the individuals*. One can reasonably argue that such an approach is not suitable for vibration serviceability assessment traditionally done by hand. However, it could be coded and used as a toolbox within a commercial FEM software, which any way would be utilised to estimate modal properties of a structure at the design stage. This fully computerized vibration serviceability assessment could be carried out for a number of locations on the structure, thus creating a vibration performance map which would identify critical points in the design. A standard PC could complete such analysis within minutes making the design more reliable and potentially less costly. However, there is a single missing ingredient to realize this ambition. A comprehensive database of experimentally measured motion trajectories of a large number of individuals moving in groups of various sizes, prompted under a range of different stimuli and performing different actions (e.g. walking, jumping, running), is needed to identify realistic values of the modelling parameters and study their natural variation within the human population. To the best knowledge of the authors, such a database is at present not available anywhere in the world.

Acknowledgements. The first author is partially supported by the PRIN project *Equazioni alle derivate parziali di tipo ellittico e parabolico: aspetti geometrici, disuguaglianze collegate, e applicazioni* and by the Gruppo Nazionale per l'Analisi Matematica, la Probabilità e le loro Applicazioni (GNAMPA) of the Istituto Nazionale di Alta Matematica (INdAM). The second author would like to acknowledge the financial support of the PRIN project *Identification and monitoring of complex structural systems*. The Authors are grateful to the anonymous Reviewers for their suggestions and remarks that led to an improvement of the present paper.

References

- [1] E. Ahmadi, C.C. Caprani, A. Heidarpour, *An equivalent moving force model for consideration of human-structure interaction*, Appl. Math. Modelling 51, 526-545 (2017)
- [2] G. Arioli, F. Gazzola, *A new mathematical explanation of what triggered the catastrophic torsional mode of the Tacoma Narrows Bridge collapse*, Appl. Math. Modelling 39, 901-912 (2015)
- [3] R.C. Batista, C. Magluta, *Spectator-induced vibration of Maracan football stadium*, Proceedings of the 2nd European Conference on Structural Dynamics EURO-DYN 93, Trondheim, Norway, 21-25 June (1993)
- [4] E. Berchio, F. Gazzola, C. Zanini, *Which residual mode captures the energy of the dominating mode in second order Hamiltonian systems?*, SIAM J. Appl. Dynam. Syst. 15, 338-355 (2016)
- [5] M. Bocian, J.M.W. Brownjohn, V. Racic, D. Hester, A. Quattrone, R. Monnickendam *Framework for experimental identification of localised vertical pedestrian forces on full-scale structures using wireless inertial sensors*, J. Sound Vibr. 376, 217-243 (2016)

- [6] M. Bocian, J. Macdonald, J. Burn, *Biomechanically-inspired modelling of pedestrian-induced vertical self-excited forces*, ASCE J. Bridge Engin. 18(12), 1336-1346 (2012)
- [7] BS 6399-1:1996, *Loading for buildings*, British Standard Institution, London, UK (1996)
- [8] Canadian Commission on Building and Fire Codes, *Users Guide NBC 2005: Structural Commentaries (Part 4 of Division B)*. National Research Council of Canada, Institute for Research in Construction, Ottawa, Canada (2006)
- [9] C.C. Caprani, E. Ahmadi, *Formulation of human-structure interaction system models for vertical vibration*, J. Sound Vibr. 377, 346-367 (2016)
- [10] C.C. Caprani, E.J. OBrien, A. Lipari, *Long-span bridge traffic loading based on multi-lane traffic micro-simulation*, Eng. Structures 115, 207-219 (2016)
- [11] S.P. Carroll, J.S. Owen, M.F.M. Hussein, *Modelling crowd-bridge dynamic interaction with a discretely defined crowd*, J. Sound Vibr. 331(11), 2685-2709 (2012)
- [12] L. Cesari, *Asymptotic behavior and stability problems in ordinary differential equations*, Springer, Berlin (1971)
- [13] C. Chicone, *Ordinary differential equations with applications*, Texts in Applied Mathematics 34, 2nd Edition, Springer, New York (2006)
- [14] A.J. Comer, M.S. Williams, A. Blakeborough, *Experimental determination of crowd load and coherency when jumping on a rigid raked grandstand*, IMAC XXV: 25th International Modal Analysis Conference, Orlando, Florida, USA, 19-22 Feb. (2007)
- [15] A. Ebrahimpour, L.L. Fitts, *Measuring coherency of human-induced rhythmic loads using force plates*, ASCE J. Struct. Engin. 122(7), 829-831 (1996)
- [16] B.R. Ellis, T. Ji, *The response of structures to dynamic crowd loads*, BRE Digest, 426, London, UK (1997)
- [17] A. Ferrarotti, F. Tubino, *Generalized equivalent spectral model for serviceability analysis of footbridges*, J. Bridge Engin. 21(12), 04016091 (2016)
- [18] T. Fitzpatrick, P. Dallard, S. Le Bourva, A. Low, R. Ridsdill-Smith, M. Willford, *Linking London: the Millennium Bridge*, Report No. L12.32. The Royal Academy of Engineering, London, UK (2001)
- [19] F. Gazzola, *Mathematical models for suspension bridges*, MS&A Vol. 15, Springer (2015)
- [20] G.W. Hill, *On the part of the motion of the lunar perigee which is a function of the mean motions of the sun and the moon*, Acta Math. 8, 1-36 (1886)
- [21] E.T. Ingolfsson, C.T. Georgakis, *A stochastic load model for pedestrian-induced lateral forces on footbridges*, Engin. Struct. 33(12), 3454-3470 (2011)
- [22] ISO (International Organization for Standardization). *Bases for design of structures-serviceability of buildings and walkways against vibration*, ISO 10137, Geneva. Switzerland (2007)
- [23] IStructE/DCLG/DCMS Working Group, *Dynamic performance requirements for permanent grandstands subject to crowd action: Recommendations for management, design and assessment*, The Institution of Structural Engineers, London, UK (2008)
- [24] C.A. Jones, P. Reynolds, A. Pavic, *Vibration serviceability of stadia structures subjected to crowd loads: a literature review*, J. Sound Vibr. 330 (8) 1531-1566 (2011)
- [25] M. Kasperski, E. Agu, *Prediction of crowd-induced vibrations via simulation*, IMAC XXIII: Proceedings of 23rd International Modal Analysis Conference, Orlando, Florida, USA, 31st Jan - 3rd Feb (2005)
- [26] W. Lacarbonara, *Nonlinear structural mechanics*, Springer (2013)
- [27] S-H. Lee, K-K. Lee, S-S. Woo, S-H. Cho, *Global vertical mode vibrations due to human group rhythmic movement in a 39 story building structure*, Engin. Struct. 57, 296-305 (2013)
- [28] G. Luck, J.A. Sloboda, *Spatio-temporal cues for visually mediated synchronization*. Music Perception 26(5), 465-473 (2009)

- [29] J. Macdonald, *Lateral excitation of bridges by balancing pedestrians*, Proceedings of the Royal Society A - Math. Phys. Engin. Sci. 465, 1055-1073 (2009)
- [30] W. Magnus, S. Winkler, *Hill's equation*, Dover, New York (1979)
- [31] N.W. McLachlan, *Theory and application of Mathieu functions*, Dover Publications, New York (1964)
- [32] G. Piccardo, F. Tubino, *Equivalent spectral model and maximum dynamic response for the serviceability analysis of footbridges*, Engin. Struct. 40, 445-456 (2012)
- [33] V. Racic, J.M.W. Brownjohn, *Stochastic model of near-periodic vertical loads due to humans walking*, Adv. Engin. Informatics 25(2), 259-275 (2011)
- [34] V. Racic, J.M.W. Brownjohn, *Mathematical modelling of random narrow band lateral excitation of footbridges due to pedestrians walking*, Computers & Structures 90-91, 116-130 (2012)
- [35] V. Racic, J.M.W. Brownjohn, A. Pavic, *Reproduction and application of human bouncing and jumping forces from visual marker data*, J. Sound Vibr. 329, 3397-3416 (2010)
- [36] V. Racic, J. Chen, *Data-driven generator of stochastic dynamic loading due to people bouncing*, Computers and Structures 158, 240-250 (2015)
- [37] V. Racic, A. Pavic, *Stochastic approach to modelling near-periodic jumping force signals*, Mech. Syst. Signal Process. 24, 3037-3059 (2010)
- [38] J.H. Rainer, G. Pernica, D.E. Allen, *Dynamic loading and response of footbridges*, Canadian J. Civil Engin. 15 (1), 66-71 (1988)
- [39] L. Ruby, *Applications of the Mathieu equation*, American J. Phys. 64, 39-44 (1996)
- [40] Sétra/AFGC, *Passerelles piétonnes. Évaluation du comportement vibratoire sous l'action des piétons*. (Footbridges. Assessment of vibrational behaviour of footbridges under pedestrian loading), Paris, France (2006)
- [41] J.H.H. Sim, A. Blakeborough, M. Williams, *Statistical model of crowd jumping loads*, ASCE J. Struct. Engin. 134(12), 1852-1861 (2008)
- [42] S. Strogatz, *Sync: The emerging science of spontaneous order*, Hyperion, New York, USA (2003)
- [43] K. Van Nimmen, G. Lombaert, I. Jonkers, G. De Roeck, P. Van den Broeck, *Characterisation of walking loads by 3D inertial motion tracking*, J. Sound Vibr. 333, 5212-5226 (2014)
- [44] K. Van Nimmen, G. Lombaert, G. De Roeck, P. Van den Broeck, *Vibration serviceability of footbridges: Evaluation of the current codes of practice*, Engin. Struct. 59, 448-461 (2014)
- [45] F. Venuti, V. Racic, A. Corbeta, *Modelling framework for dynamic interaction between multiple pedestrians and vertical vibrations of footbridges*, J. Sound Vibr. 379, 245-263 (2016)
- [46] F. Venuti, L. Bruno, *Crowd-structure interaction in lively footbridges under synchronous lateral excitation: A literature review*, Phys. Life Rev. 6(3), 176-206 (2009)
- [47] S. Zivanovic, A. Pavic, *Probabilistic modelling of walking excitation for building floors*, J. Perform. Constr. Facilities 23(3), 132-43 (2009)
- [48] S. Zivanovic, A. Pavic, P. Reynolds, *Human-structure dynamic interaction in footbridges*, Bridge Engin. 158 (BE4), 165-177 (2005)